Interpatient Variation in Normal Peripheral Zone Apparent Diffusion Coefficient: Effect on the Prediction of Prostate Cancer Aggressiveness[1]

Geert J. S. Litjens, MSc
Thomas Hambrock, MD
Christina Hulsbergen–van de Kaa, MD, PhD
Jelle O. Barentsz, MD, PhD
Henkjan J. Huisman, PhD

Purpose: To determine the interpatient variability of prostate peripheral zone (PZ) apparent diffusion coefficient (ADC) and its effect on the assessment of prostate cancer aggressiveness.

Materials and Methods: The requirement for institutional review board approval was waived. Intra- and interpatient variation of PZ ADCs was determined by means of repeated measurements of normal ADCs at three magnetic resonance (MR) examinations in a retrospective cohort of 10 consecutive patients who had high prostate-specific antigen levels and negative findings at transrectal ultrasonographically-guided biopsy. In these patients, no signs of PZ cancer were found at all three MR imaging sessions. The effect of interpatient variation on the assessment of prostate cancer aggressiveness was examined in a second retrospective cohort of 51 patients with PZ prostate cancer. Whole-mount step-section pathologic evaluation served as reference standard for placement of regions of interest on tumors and normal PZ. Repeated-measures analysis of variance was used to determine the significance of the interpatient variations in ADCs. Linear logistic regression was used to assess whether incorporating normal PZ ADCs improves the prediction of cancer aggressiveness.

Results: Analysis of variance revealed that interpatient variability (1.2–2.0 $\times 10^{-3}$ mm^2/sec) was significantly larger than measurement variability (0.068 $\times 10^{-3}$ mm^2/sec $\pm$ 0.027 [standard deviation]) (P = .0058). Stand-alone tumor ADCs showed an area under the receiver operating characteristic curve (AUC) of 0.91 for discriminating low-grade versus high-grade tumors. Incorporating normal PZ ADC significantly improved the AUC to 0.96 (P = .0401).

Conclusion: PZ ADCs show significant interpatient variation, which has a substantial effect on the prediction of prostate cancer aggressiveness. Correcting this effect results in a significant increase in diagnostic accuracy.

[1] From the Department of Radiology, Radboud University Nijmegen Medical Centre, Geert Grooteplein 10, 6525 GA Nijmegen, the Netherlands. Received November 23, 2011; revision requested January 23, 2012; revision received March 20; accepted April 16; final version accepted April 24. **Address correspondence to** G.J.S.L. (e-mail: *g.litjens@rad.umcn.nl*).

Only 15% of men diagnosed with prostate cancer show a disease-specific mortality. The mortality in the United States in 2010 was 30000, with 220000 new cases of prostate cancer diagnosed (1). Thus, to tailor treatment from more radical therapy to active surveillance protocols, accurate cancer aggressiveness risk stratification is very important. The most useful estimator of cancer aggressiveness is the Gleason score, a histopathologic scoring system used for biopsy and prostatectomy specimens. It has become such an integral part in prostate cancer evaluation that patient management is largely influenced by the assessment thereof (2–4).

Recently, the apparent diffusion coefficient (ADC) determined from diffusion-weighted magnetic resonance (MR) imaging was shown to be inversely correlated to Gleason score (5–7). As a result, ADC has been proposed as useful noninvasive biomarker for prostate cancer aggressiveness (5,7). However, the discriminative power of ADC depends in part on the variability of the ADC measurement. This variability is machine (ie, vendor, settings, noise) and patient dependent, the latter caused by natural tissue heterogeneity. On the basis of the large interpatient distribution of normal peripheral zone (PZ) ADCs (1.2–2.2 $\times 10^{-3}$ mm^2/sec) observed at a single MR imager, we hypothesize that a substantial histophysiologic heterogeneity between patients must exist (interpatient variation) (7,8).

Interpatient ADC variation could affect the discriminative power of ADC both for prostate cancer localization and for the determination of prostate cancer aggressiveness. Since normal prostate PZ tissue fluctuates significantly in ADC, the ADCs of an aggressive tumor may show similar fluctuations. If normal PZ and tumor ADC are correlated, considering both simultaneously may lead to better estimates of aggressiveness.

The purpose of this study was to determine the interpatient variability of prostate PZ ADCs at 3-T MR imaging and the effect this has on the assessment of prostate cancer aggressiveness.

Advances in Knowledge

- Large interpatient variability exists for normal peripheral zone apparent diffusion coefficients (1.2–2.0 $\times 10^{-3}$ mm^2/sec) derived from diffusion-weighted MR imaging at 3 T; this interpatient variability is significant (P = .0058).
- Correcting for interpatient variability results in a significant increase in diagnostic accuracy for separating low-grade and high-grade cancer (area under the receiver operating characteristic curve: from 0.91 to 0.96; P = .0401).
- A clinically useful nomogram is created that may aid radiologists in improving their assessment of prostate cancer aggressiveness.

Materials and Methods

Patients

Imaging data of two retrospective patient cohorts were used in our experiments. The requirement to obtain institutional review board approval was waived for both cohorts because this study does not fall within the remit of the Medical Research Involving Human Subjects Act. Therefore, our study could be performed in the Netherlands without an approval by an accredited research ethics committee. To determine the significance of the interpatient variance relative to the measurement variability, we included 10 consecutive patients (from February 2008 to June 2011; interval between imaging examinations, 6–12 months) who had undergone repeated measurements of normal PZ ADCs at three separate MR imaging sessions at 3 T. The indication for the studies was a continuously high prostate-specific antigen (PSA) level and at least one transrectal ultrasonographically-guided biopsy with negative findings. Patients were followed up if the PSA level remained high. In these patients no PZ cancer was found at all three imaging sessions by an expert radiologist (J.O.B., with 18 years of experience). If a suspicious lesion was indicated by the radiologist, subsequent MR-guided biopsy found no traces of tumor.

A second cohort was included to determine the effect of the interpatient variation of ADC on the prediction of PZ prostate cancer aggressiveness. Between August 2006 and January 2009, 70 consecutive patients with biopsy-proven PZ prostate cancer, scheduled to undergo radical prostatectomy, were referred from the departments of urology at the Radboud University Nijmegen Medical Centre and the Canisius Wilhelmina Hospital in Nijmegen, the Netherlands, for clinically routine preoperative MR imaging of the prostate (7). Figure 1 details the inclusion of patients in flow charts.

MR Imaging Protocol

MR imaging of the prostate was performed by using a 3-T MR imager (Trio Tim; Siemens, Erlangen, Germany). The first cohort of 10 patients was imaged with only the pelvic phased-array coils.

The second cohort was imaged with the use of combined endorectal coil

Published online before print
10.1148/radiol.12112374 **Content code:** GU

Radiology 2012; 265:260–266

Abbreviations:
ADC = apparent diffusion coefficient
PSA = prostate-specific antigen
PZ = peripheral zone
ROC = receiver operating characteristic
ROI = region of interest

Author contributions:
Guarantors of integrity of entire study, G.J.S.L., J.O.B., H.J.H.; study concepts/study design or data acquisition or data analysis/interpretation, all authors; manuscript drafting or manuscript revision for important intellectual content, all authors; approval of final version of submitted manuscript, all authors; literature research, T.H., H.J.H.; clinical studies, C.H.v.d.K., J.O.B.; experimental studies, T.H., H.J.H.; statistical analysis, G.J.S.L., H.J.H.; and manuscript editing, G.J.S.L., T.H., J.O.B., H.J.H.

Potential conflicts of interest are listed at the end of this article.

(Medrad, Pittsburgh, Pa) and pelvic phased-array coils. The endorectal coil was filled with a 40-mL perfluorocarbon preparation (Fomblin, Solvay-Solexis, Milan, Italy).

In both cohorts peristalsis was suppressed with an intramuscular administration of 20 mg butylscopolaminebromide (Buscopan; Boehringer-Ingelheim, Ingelheim, Germany) and 1 mg of glucagon (Glucagen; Nordisk, Gentofte, Denmark).

The MR imaging protocol included in anatomic T2-weighted turbo spin-echo sequences in axial, sagittal, and coronal planes covering the entire prostate and seminal vesicles. Axial diffusion-weighted imaging was performed by using a single-shot echo-planar imaging sequence with diffusion modules and fat suppression pulses implemented. Water diffusion was measured in three-scan trace mode by using *b* values of 0, 50, 500, and 800 sec/mm^2. ADC maps were automatically calculated by the imager software by using all *b* values. Complete pulse sequence details can be found in Table 1 for the first cohort containing 10 patients with repeated measurements and Table 2 for the second cohort.

Reconstructed Whole-Mount Step-Section Preparation

The second cohort of patients underwent radical prostatectomy after imaging. After the radical prostatectomy, prostate specimens were uniformly processed and entirely submitted for histologic investigation. After histologic staining, all specimens were evaluated by one expert urologic pathologist (C.A.H.v.d.K., with 17 years of experience). Each individual tumor was graded according to the 2005 International Society of Urological Pathology Modified Gleason Grading System (9).

PZ tumors, with a size of greater than 0.5 mL in volume, were divided in two groups and classified as low- and high-grade tumors. Tumors with a Gleason grade 4 or 5 component were defined as high-grade tumors. Low-grade tumors were defined as tumors harboring only Gleason grades 2 and 3.

Figure 1

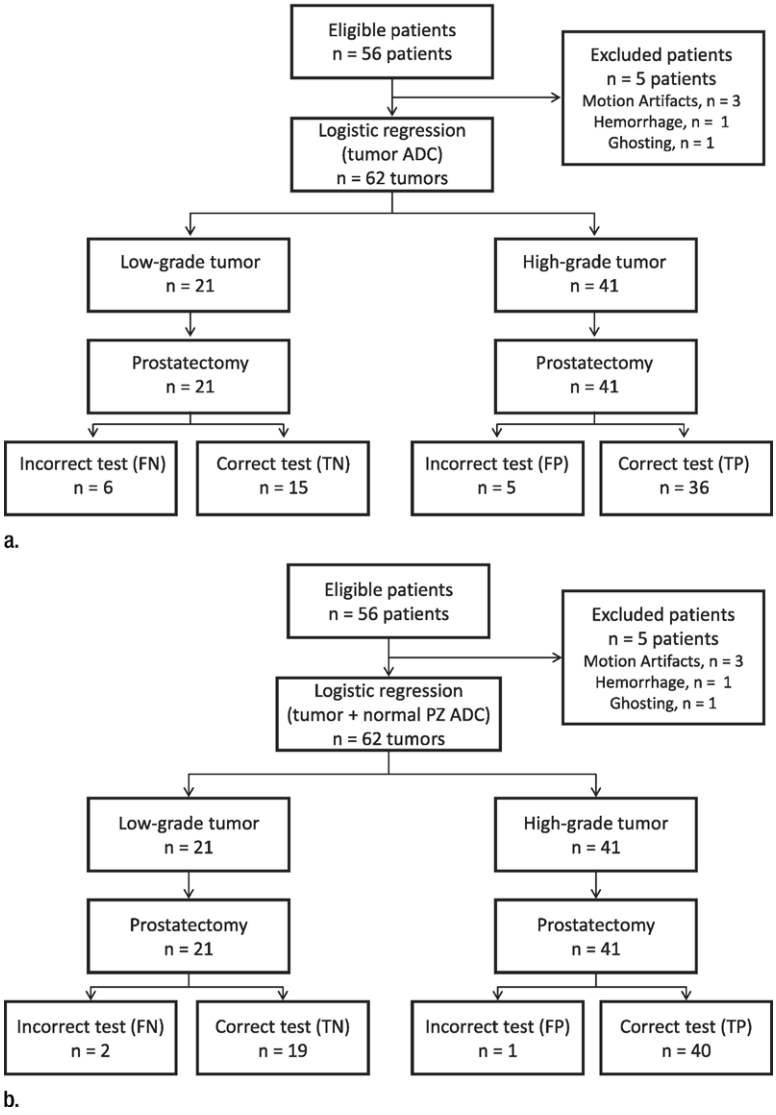

Figure 1: Flowcharts expressing the diagnostic accuracy of **(a)** the method including only tumor ADC and **(b)** the method incorporating both tumor and normal PZ ADC. *FN* = false negative, *FP* = false positive, *TN* = true negative, *TP* = true positive.

Annotation of MR Images

All annotations were performed by using an MR viewing and reporting system developed in-house. In the first cohort the center section of the prostate in the axial direction was used to annotate the PZ. For this section the whole PZ was annotated and the median ADC was extracted from this annotation.

For the second cohort, ADC maps were acquired in the same orientation and of similar thickness as the histopathologic step-section. A previously described translation technique was used to match every tumor containing histopathologic step-section to a corresponding ADC map (7). With histopathologic examination used as the reference standard, a region of interest (ROI) was placed by one radiologist (T.H., with 4 years of experience) and one urologist (1 year of experience) in consensus on the ADC maps. The size and extent of the ROI were chosen such

Table 1

Pulse Sequence Details for the First Patient Cohort with Repeated Measurements

Sequence	Sequence Type	Section Thickness (mm)	No. of Sections	In-plane Resolution (mm)	TR (msec)	TE (msec)	Signals Acquired	GRAPPA	*b* Values (mm²/sec)
T2-weighted axial	TSE	3.5–4	13–19	0.6	3540	104	2–3		
T2-weighted coronal	TSE	3.5–4	15–19	0.6–0.8	3350	105	2–3		
T2-weighted sagittal	TSE	3.5–4	15–19	0.6–0.8	3810	105	2–3		
Diffusion weighted	SE-EPI	3.5–4	15–20	1.6–2.0	2300	61	6–10	2	0, 50, 500, 800
T1-weighted dynamic contrast enhanced	GRE (FLASH 3D)	3.5–4	14	1.8	37	1.47	1		

Note.—In-plane resolution is the same in both directions. FLASH 3D = fast low-angle shot three dimensional, GRAPPA = generalized autocalibrating partially parallel acquisition, GRE = gradient-recalled echo, SE-EPI = spin-echo echo-planar imaging, TE = echo time, TR = repetition time, TSE = turbo spin echo.

Table 2

Pulse Sequence Details for the Second Patient Cohort

Sequence	Sequence Type	Section Thickness (mm)	No. of Sections	In-plane Resolution	TR (msec)	TE (msec)	Signals Acquired	GRAPPA	*b* Values (mm²/sec)
T2-weighted axial	TSE	4	15–19	0.4	3540	104	2		
T2-weighted coronal	TSE	4	15–19	0.5	3350	105	2		
T2-weighted sagittal	TSE	4	15–19	0.5	3810	105	2		
Diffusion weighted	SE-EPI	4	15–19	2.0	2800	81	10	2	0, 50, 500, 800
T1-weighted dynamic contrast enhanced	GRE (FLASH 3D)	4	14	1.8	37	1.47	1		

Note.—In-plane resolution is the same in both directions. FLASH 3D = fast low-angle shot three dimensional, GRAPPA = generalized autocalibrating partially parallel acquisition, GRE = gradient-recalled echo, SE-EPI = spin-echo echo-planar imaging, TE = echo time, TR = repetition time, TSE = turbo spin echo.

that it matched the tumor size and extent obtained from histologic examination as closely as possible. Median ADCs were extracted for each tumor section separately. In clinical practice, the ADC section revealing the lowest signal intensity for tumor alerts radiologists. Therefore, for each individual PZ tumor, the tumor section revealing the lowest ADCs was used for further assessment (7).

Last, to determine the effect of incorporating normal PZ ADCs in the prediction of cancer aggressiveness, an ROI was placed in the normal PZ tissue of every patient. This region was always selected adjacent to the tumor, to be the most representative area of normal PZ ADC at the tumor location. This was done to attempt to minimize intrapatient heterogeneity. Median ADCs were extracted from all ROIs. Median values were used because they are more robust to image artifacts that might occur due to ADC calculation by the imager.

Statistical Analysis

Our first hypothesis was that there is a significant degree of interpatient variation in normal PZ ADCs. This was assessed by using a repeated-measures analysis of variance. Mauchly sphericity test was performed to test the hypothesis of sphericity. If sphericity could be assumed the Greenhouse-Geisser corrected *P* value was reported. The repeated measure was the median ADC of normal PZ tissue, which was obtained three times for each of the 10 patients in the first cohort.

Our second hypothesis was that joint analysis of the normal PZ ADCs and the tumor ADCs will result in an improved prediction of cancer aggressiveness, because this implicitly corrects for the interpatient variations in normal PZ ADC. Multivariate linear logistic regression was used to test this hypothesis. We can express a regression model of cancer grade as follows:

$$z = C + \beta_T ADC_T + \beta_N ADC_N \quad (1)$$

$$p = \frac{e^z}{1 + e^z} \quad (2).$$

The p indicates the probability that a cancer is high grade and the ADC variables indicate the median ADC of the corresponding ROI. Subscripts T and N are tumor and normal PZ, respectively. The β terms are the regression coefficient corresponding to these variables. Equation (2) represents the conversion from z to the probability p.

The linear logistic regression results in values for β_T and β_N and the significance of these variables in the regression model. Two regression models were created to compare diagnostic performance: one model using only tumor ADCs and one using tumor and normal PZ ADCs. SPSS (version 16.0.01; SPSS, Chicago, Ill) was used for the statistical

Table 3

Clinical and Pathologic Characteristics for the Second Patient Cohort

Characteristic	Finding
No. of patients	51
Clinical characteristics*	
PSA level (ng/mL)	6.8 (1.7–42)
Age (y)	64 (49–69)
Pathologic characteristics (per patient)	
Stage T2a	5
Stage T2c	23
Stage T3a	18
Stage T3b	4
Stage T4	1
Gleason grade (per tumor)	
3 + 2	3
3 + 3	18
2 + 4	1
3 + 4	13
3 + 4 + 5	4
4 + 3	13
4 + 3 + 5	5
4 + 4	2
4 + 5	3

* Data are the mean, and numbers in parentheses are the range.

Figure 2

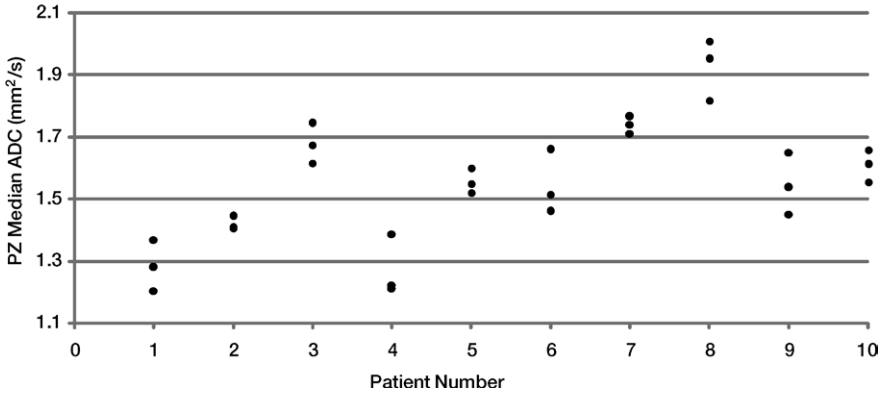

Figure 2: Three median ADC measurements of the PZ of 10 patients. The black dots represent the individual measurements, the vertical axis shows the median ADC, and the horizontal axis shows to which patient the measurement belongs.

analysis. Furthermore, a visual assessment is given for the correlation between tumor ADC and normal PZ ADC by plotting the low- and high-grade tumors with respect to their ADCs and the corresponding normal PZ ADCs.

Our third hypothesis was that the improved prediction of prostate cancer aggressiveness may result in a significant improvement in diagnostic accuracy in separating low- and high-grade cancer. Receiver operating characteristic (ROC) curves were constructed for a standalone tumor ADC regression model and the regression model, which incorporates normal PZ ADCs. The areas under the ROC curves were tested for significant differences by using the Rockit software package (Kurt Rossmann Laboratories, University of Chicago, Chicago, Ill) (10).

Nomogram Construction

Additionally, the regression model incorporating tumor and normal PZ ADC was used to construct a nomogram by evaluating the obtained equation for a range of ADCs. The ranges used to construct the nomogram were 0.5–1.7 $\times 10^{-3}$ mm^2/sec for the tumor ADC and 0.8–2.2 $\times 10^{-3}$ mm^2/sec for the normal PZ ADC. These ranges are slightly larger than the ranges found in this study to accommodate more extreme values.

Results

For the first cohort of 10 patients, no patients were excluded. The median patient age was 58.5 years (47–67 years). The median PSA level at the time of the first MR imaging was 8.25 (1.8–26).

For the second cohort of 70 consecutive patients, 56 patients had a clinically important tumor (> 0.5 mL). Of the remaining 14 patients, 11 had a tumor in the central gland and three had a PZ tumor smaller than 0.5 mL. Of the 56 patients, five patients were excluded due to severe motion artifacts (n = 3), hemorrhage (n = 1), or ghosting (n = 1). Characteristics of these patients are reported in Table 3. In the remaining 51 patients, a total of 62 different PZ tumors were found. Of these tumors, 21 were low-grade tumors and 41 were high-grade tumors. The mean ADC for the low-grade tumors was 1.35 $\times 10^{-3}$ mm^2/sec ± 0.26 (standard deviation) and for the high-grade tumors was 0.926 $\times 10^{-3}$ mm^2/sec ± 0.18. The mean value of the normal PZ for patients with a low-grade tumor was 1.65 $\times 10^{-3}$ mm^2/sec ± 0.21 and 1.60 $\times 10^{-3}$ mm^2/sec ± 0.21 for patients with a high-grade tumor.

Assessment of Interpatient Variation in Normal PZ ADCs

Normal PZ ADCs differed significantly between patients relative to measurement variability (Mauchly sphericity test, $P < .0001$; Greenhouse-Geisser corrected P value, $P = .0058$) as assessed by using the repeated-measures analysis of variance. The ADC measurements are plotted in Figure 2.

Effect of Including Normal PZ ADCs in the Prediction of Cancer Aggressiveness

Normal PZ ADC correlates with ADC of high-grade tumors. Its addition to the regression model results in a significantly improved prediction of aggressiveness ($P = .013$). This was determined by using the logistic regression procedure; the results are summarized in Table 4.

Both regression models show a significant contribution of the tumor ADC ($P = .003$). Normal PZ ADCs also show a significant contribution to the regression model ($P = .013$).

The regression model using standalone tumor ADCs can then be expressed as

$$z = 10.76 - 9.103 ADC_T \qquad (3),$$

and the model combining tumor and normal PZ ADCs can be expressed as

$$z = 0.126 - 18.82ADC_T + 13.43ADC_N \quad (4).$$

In combination with Equation (2), these models result in a probability that a given sample is a high-grade cancer. The model incorporating normal PZ ADC (Eq [4]), together with the data used in the regression, is shown in Figure 3. This plot indicates that a relatively high tumor ADC might still constitute a high-grade tumor if the normal PZ ADC is high. In addition, one can appreciate that using a static threshold on tumor ADC (a vertical line/contour in Fig 3) to determine cancer aggressiveness could result in incorrect diagnosis in some patients.

Diagnostic Performance of the Regression Models

Including normal PZ significantly (P = .0401) improved diagnostic accuracy. The ROC curves for the regression models in Equations 3 and 4 are shown in Figure 4. The area under the curve increases from 0.91 to 0.96. We have also included flow charts detailing the diagnostic accuracy of both tests in Figure 1.

Nomogram

The constructed nomogram is shown in Figure 5. This nomogram can be used in a clinical setup to quickly look up the change of a certain region with the PZ being an aggressive cancer.

Table 4

Results of Linear Logistic Regression for Three Regressions Based on Equations (1) and (2)

	Tumor Median ADC		Tumor and Normal PZ Median ADC	
Parameter	Value	*P* Value	Value	*P* Value
β_T	9.103	.000	−18.82	.003
β_N	—	—	13.43	.013
C	10.76	.000	0.126	.978

Note.—Table shows regressions performed by using only tumor ADC and by using tumor and normal PZ median ADC. The β parameters are regression parameters and their value and significance are shown respectively for each regression. Subscripts *T* and *N* = tumor and normal PZ tissue, respectively. *C* = regression constant.

Figure 3

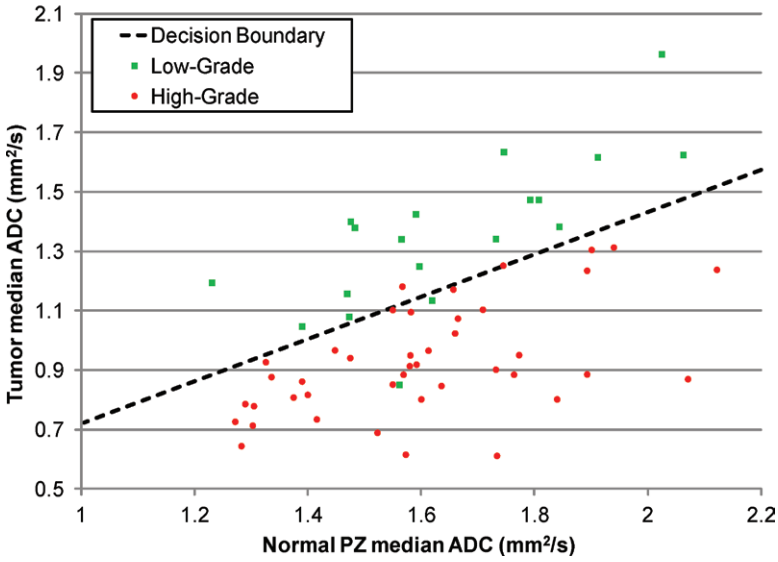

Figure 3: Decision Boundary at P = .5 of the logistic regression model. The line represents the decision boundary, the green dots the low-grade cancer, and the red dots the high-grade cancers.

Discussion

In this study we have shown that there is significant interpatient variation in normal PZ ADCs (1.2–2.0 $\times 10^{-3}$ mm^2/sec), which cannot be solely attributed to measurement variability (average measurement, 0.068×10^{-3} mm^2/sec ± 0.027 [standard deviation]). We hypothesize that the interpatient variations arise from natural variations in prostate physiology. Normal PZ ADC mean and standard deviation were comparable between patients imaged with only a pelvic phased- array coil (first cohort) and patients imaged with an endorectal coil (second cohort): mean ADC for the first cohort was 1.60 $\times 10^{-3}$ mm^2/sec ± 0.18 and for the second cohort was 1.61 $\times 10^{-3}$ mm^2/sec ± 0.22.

Second, adding normal PZ ADCs to the linear logistic regression results in a significantly improved prediction of cancer aggressiveness (P = .013). This suggests that tumor ADCs should not be considered absolute but that these values are influenced by "background" variation of normal PZ tissue composition.

Third, the improvement also results in an increased area under the ROC curve, from 0.91 to 0.96 ($P < .05$), and thus an improved diagnostic accuracy.

This study had a number of limitations. First, the use of ADC to assess aggressiveness of transition zone tumors has not been investigated in this study. Second, this study was limited to the PZ. This was done because it is known that ADC in PZ and transition zone tumors can differ substantially. However, the majority of prostate tumors arise in the PZ. Third, the annotation of ROIs was performed by a single observer; the effect of the interobserver variability on the regression model was not assessed. In addition, placement of the

Figure 4

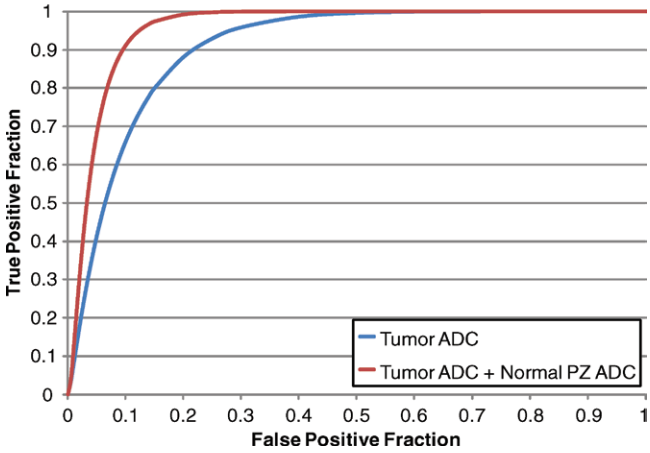

Figure 4: ROC curve of the regression models. The red line shows the diagnostic accuracy when including the adjacent PZ tissue median ADC in addition to the tumor ADC. The blue line shows the diagnostic accuracy when only using tumor ADC.

Figure 5

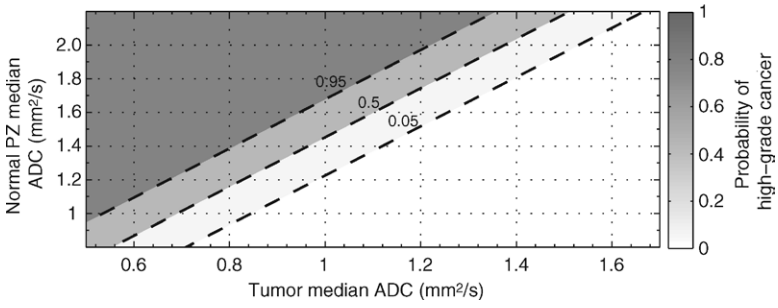

Figure 5: Contour of the probabilities of having an aggressive cancer given the adjacent PZ tissue ADC (vertical axis) and the tumor ADC (horizontal axis). The point corresponding to these two values will correspond to the probability of a high-grade cancer. The probability values are specified along the contours and in the bar on the right of the figure.

ROIs might have been influenced by the fact that the readers were not blinded to the histopathologic findings. Fourth, our nomogram must be tested and validated in a prospective multireader study. Fifth, the inclusion criteria for the first cohort included high PSA level. The high PSA level might influence the ADC of the PZ; however, the effect of the PSA level on the ADC was not investigated in this study.

In conclusion, PZ ADCs show a significant interpatient variation, which has a significant effect on the prediction of prostate cancer aggressiveness. Correcting this effect results in a significant increase (from 0.91 to 0.96 area under the ROC curve, $P = .0401$) in diagnostic accuracy.

Disclosures of Potential Conflicts of Interest: G.J.S.L. Financial activities related to the present article: Dutch Cancer Society (KWF) grant to institution (grant KUN2007-3971). Financial activities not related to the present article: none to disclose. Other relationships: none to disclose. **T.H.** No potential conflicts of interest to disclose. **C.H.v.d.K.** No potential conflicts of interest to disclose. **J.O.B.** Financial activities related to the present article: none to disclose. Financial activities not related to the present article: grant to institution from Dutch Cancer Society (KWF). Other relationships: none to disclose. **H.J.H.** Financial activities related to the present article: none to disclose. Financial activities not related to the present article: stock/stock options in QView Medical (small start-up in medical image analysis software). Other relationships: none to disclose.

References

1. Siegel R, Naishadham D, Jemal A. Cancer statistics, 2012. CA Cancer J Clin 2012;62(1):10–29.
2. Blute ML, Bergstralh EJ, Iocca A, Scherer B, Zincke H. Use of Gleason score, prostate specific antigen, seminal vesicle and margin status to predict biochemical failure after radical prostatectomy. J Urol 2001;165(1):119–125.
3. Egevad L, Granfors T, Karlberg L, Bergh A, Stattin P. Percent Gleason grade 4/5 as prognostic factor in prostate cancer diagnosed at transurethral resection. J Urol 2002;168(2):509–513.
4. Narain V, Bianco FJ Jr, Grignon DJ, Sakr WA, Pontes JE, Wood DP Jr. How accurately does prostate biopsy Gleason score predict pathologic findings and disease free survival? Prostate 2001;49(3):185–190.
5. Itou Y, Nakanishi K, Narumi Y, Nishizawa Y, Tsukuma H. Clinical utility of apparent diffusion coefficient (ADC) values in patients with prostate cancer: can ADC values contribute to assess the aggressiveness of prostate cancer? J Magn Reson Imaging 2011;33(1):167–172.
6. Turkbey B, Pinto PA, Mani H, et al. Prostate cancer: value of multiparametric MR imaging at 3 T for detection—histopathologic correlation. Radiology 2010;255(1):89–99.
7. Hambrock T, Somford DM, Huisman HJ, et al. Relationship between apparent diffusion coefficients at 3.0-T MR imaging and Gleason grade in peripheral zone prostate cancer. Radiology 2011;259(2):453–461.
8. Vargas HA, Akin O, Franiel T, et al. Diffusion-weighted endorectal MR imaging at 3 T for prostate cancer: tumor detection and assessment of aggressiveness. Radiology 2011;259(3):775–784.
9. Epstein JI, Allsbrook WC Jr, Amin MB, Egevad LL; ISUP Grading Committee. The 2005 International Society of Urological Pathology (ISUP) Consensus Conference on Gleason Grading of Prostatic Carcinoma. Am J Surg Pathol 2005;29(9):1228–1242.
10. Metz CE, Herman BA, Roe CA. Statistical comparison of two ROC-curve estimates obtained from partially-paired datasets. Med Decis Making 1998;18(1):110–121.